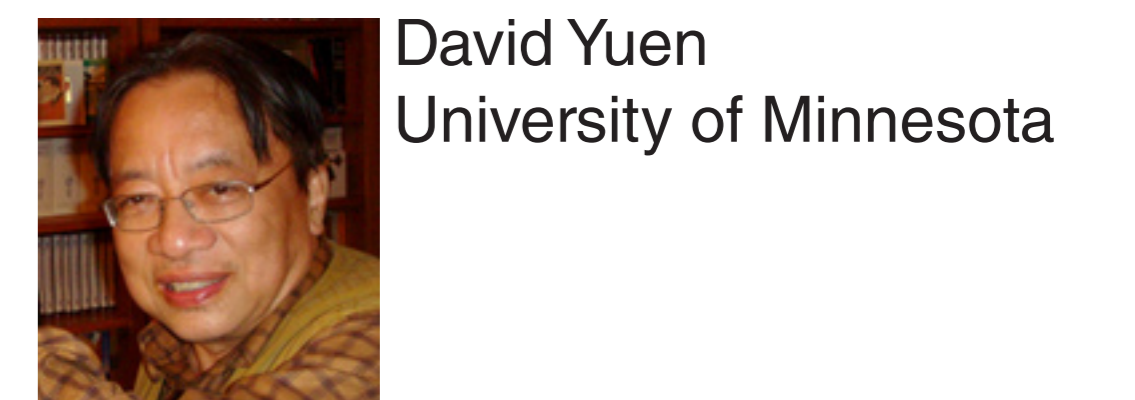
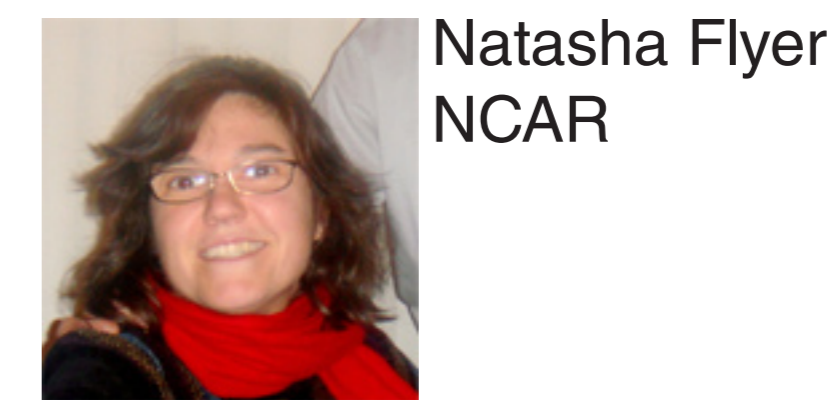


3-D Spherical Mantle Convection with Radial Basis Functions



Brief History: Numerical Methods for Mantle Convection

Late 60s: Turcotte & Torrance, 2nd order finite-difference (FD) with 20x20 nodes for variable depth-dependent viscosity with the steady-state approach

Mid 70s: Weiss & McKenzie, time-dependent convection with staggered FDs

Late 70s: Woitd & Christiansen, Bi-cubic splines were introduced

Mid 80s: French school-Toulouse, 3-D spherical convection using spherical harmonics (SH) and 2nd order FD in the radial direction

Late 80s: Glatzmaier, 3-D spherical convection problem with Chebyshev polynomials in the radial direction and SH for the angular portion.

Early 90s: Tackley, used a 2nd order finite-volume method (FV) with multigrid in 3-D Cartesian geometry for variable viscosity

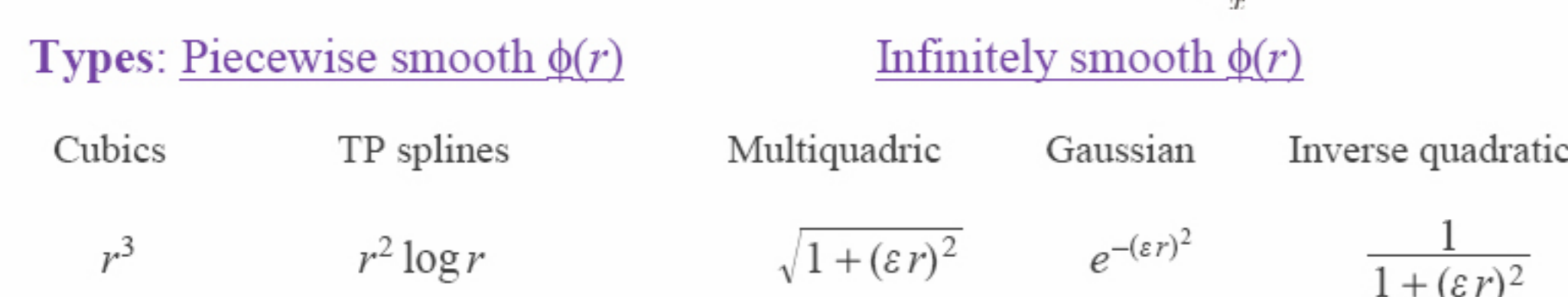
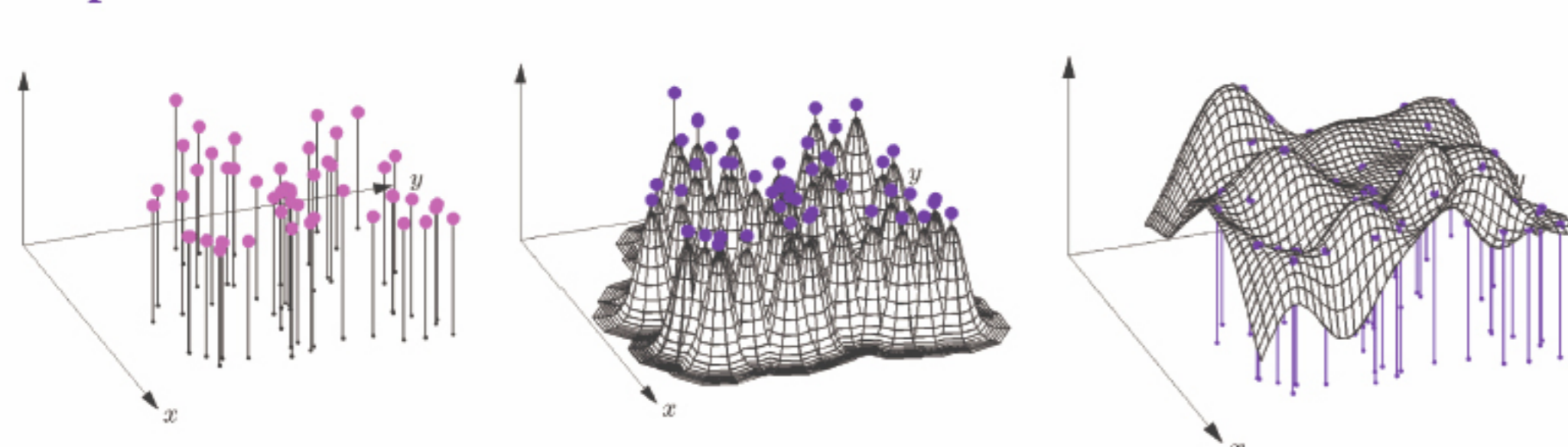
Mid 90s: Moresi, 2nd order finite-elements using a weak variational formulation

Late 90s: Extending Moresi's work to 3-D, resulting in CITCOM code-mainstay in the mantle convection community in this millennium.

Mid 00s: Kageyama, Yin-Yang grid for 3-D spherical problems with 2nd order FV

Introduction to Radial Basis Functions via Interpolation

In pictures:



In Formulas:

Given scattered data (x_k, f_k) , $k = 1, 2, \dots, N$, the coefficients λ_k in

$$s(x) = \sum_{k=1}^N \lambda_k \phi(\|x - x_k\|)$$

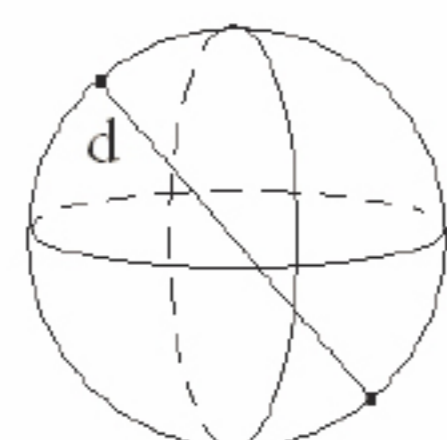
are found by collocation: $s(x_k) = f_k$, $k = 1, 2, \dots, N$:

$$\begin{bmatrix} \phi(\|x_1 - x_1\|) & \phi(\|x_1 - x_2\|) & \dots & \phi(\|x_1 - x_N\|) \\ \phi(\|x_2 - x_1\|) & \phi(\|x_2 - x_2\|) & \dots & \phi(\|x_2 - x_N\|) \\ \vdots & \vdots & \ddots & \vdots \\ \phi(\|x_N - x_1\|) & \phi(\|x_N - x_2\|) & \dots & \phi(\|x_N - x_N\|) \end{bmatrix} \begin{bmatrix} \lambda_1 \\ \lambda_2 \\ \vdots \\ \lambda_N \end{bmatrix} = \begin{bmatrix} f_1 \\ \vdots \\ f_N \end{bmatrix}$$

where $\|\cdot\|$ is the Euclidean distance between 2 nodes

For spheres:

$$d = \|x - x_k\| = \sqrt{(x-x_k)^2 + (y-y_k)^2 + (z-z_k)^2} = \sqrt{2} \sqrt{1 - \cos \theta \cos \theta_k \cos(\theta - \theta_k) - \sin \theta \sin \theta_k}$$



Advantages:

- Algorithmic **Simplicity**

Example: $\Delta_{surface} = \frac{1}{4}((4-d^2)\phi''(d) + \frac{4-3d^2}{d}\phi'(d))$

$\Delta_{surface}$ Code using Gaussian RBFs (2 lines)

```
dsq = max(2-2*(x*x' + y*y' + z*z'), 0);
L_surf = 1/4*((4-dsq)*(-2*eps^2*exp(-eps^2*dsq) + ...
2*eps^4*dsq*exp(-eps^2*dsq)) + ...
(4-3dsq)/sqrt(dsq)*(-2*eps^2*sqrt(d)*exp(-eps^2*dsq));
```

- Simplicity of Algorithm **Independent of Dimension**

d is a scalar measure between nodes that exist in n -dimensional space

- Handles Completely **Irregular Geometries** due to No Grids

- Gives **Spectral Accuracy** with Local Node **Refinement**

Thermal Convection Model in 3-D Spherical Shell

- Infinite Prandtl Number
- Constant Viscosity
- Incompressible
- Boussinesq Approximation

Momentum equation in terms of a poloidal potential Φ :

$$\left[\frac{1}{\sin \theta} \frac{\partial}{\partial \theta} \left(\sin \theta \frac{\partial}{\partial \theta} \right) + \frac{1}{\sin^2 \theta} \frac{\partial^2}{\partial \varphi^2} \right] \Phi + \frac{\partial}{\partial r} \left(r^2 \frac{\partial}{\partial r} \right) \Phi = r^2 \Omega \quad (1)$$

$$\Delta_{surface} \Omega + \frac{\partial}{\partial r} \left(r^2 \frac{\partial}{\partial r} \right) \Omega = r^2 R \alpha T \quad (2)$$

Impermeable and shear-stress free boundary conditions at $r = 0.55/0.45, 1/0.45$

$$\vec{v} = \frac{1}{r^2} \Delta_{surface} \Phi e_r + \frac{1}{r} \frac{\partial^2}{\partial r \partial \theta} \Phi e_\theta + \frac{1}{r \sin \theta} \frac{\partial^2}{\partial r \partial \theta} \Phi e_\varphi$$

Energy equation

$$\frac{\partial T}{\partial t} + \vec{v} \cdot \left(\frac{\partial}{\partial r} e_r + \frac{1}{r} \frac{\partial}{\partial \theta} e_\theta + \frac{1}{r \sin \theta} \frac{\partial}{\partial \varphi} e_\varphi \right) T = \frac{1}{r^2} \left[\Delta_{surface} + \frac{\partial}{\partial r} \left(r^2 \frac{\partial}{\partial r} \right) \right] T$$

$T = 1$ at $r = 0.55/0.45$, $T = 0$ at $r = 1/0.45$

Algorithm:

- Discretize $\Delta_{surface}$, $\frac{\partial}{\partial \theta}$, $\frac{\partial}{\partial \varphi}$ using **RBFs**
- Discretize $\frac{\partial}{\partial r}$, $\frac{\partial^2}{\partial r^2}$ using **Chebyshev polynomials**
- Discretize time using a **time-splitting** scheme
 - 2nd order Adams-Moulton (AM2) in radial direction (**implicit**)
 - 3rd order Adams-Bashforth (AB3) in angular portion (**explicit**)
- Time-step energy equation to get T^{n+1} - solution at time step $n+1$
- Use T^{n+1} solution to solve for Ω^{n+1} in (2)
- Use Ω^{n+1} solution to solve for Φ^{n+1} in (1)
- Use Φ^{n+1} solution to calculate \vec{v}^{n+1}
- Use \vec{v}^{n+1} in energy equation to calculate T at next time step

Poisson Solver

Continuous: $\left(\Delta_{surface} + \frac{\partial}{\partial r} \left(r^2 \frac{\partial}{\partial r} \right) \right) \Omega = r^2 R \alpha T$

Discrete: $S \quad R \quad \Omega \quad T$
(RBF) (Chebyshev)

Do not directly invert Laplace operator, use eigenvector decomposition of matrix

$$S = P \Lambda_S P^{-1}, \quad R = Q \Lambda_R Q^{-1}$$

After some matrix algebra:

$$(\mathbf{I}_M \otimes \Lambda_S + \Lambda_R \otimes \mathbf{I}_N) \mathbf{P}^{-1} \vec{\Omega} \mathbf{Q} = \mathbf{P}^{-1} \vec{T} \mathbf{Q}$$

Diagonal

Likewise,

$$(\mathbf{I}_M \otimes \Lambda_S + \Lambda_R \otimes \mathbf{I}_N) \mathbf{P}^{-1} \vec{\Phi} \mathbf{Q} = \mathbf{P}^{-1} \vec{\Omega} \mathbf{Q}$$

Operation Count: $O(N^2 M^2 + M^2 N^2)$ instead of $O(N^3 M^3)$

Time-Stepping Scheme

$$\frac{\partial T}{\partial t} = -\vec{v} \cdot \left(\frac{\partial}{\partial r} e_r + \frac{1}{r} \frac{\partial}{\partial \theta} e_\theta + \frac{1}{r \sin \theta} \frac{\partial}{\partial \varphi} e_\varphi \right) T + \frac{1}{r^2} \Delta_{surface} T + \frac{1}{r^2} \frac{\partial}{\partial r} \left(r^2 \frac{\partial}{\partial r} \right) T$$

$f(T, t)$ - explicit $g(T, t)$ - implicit

In discrete form:

$$T^{n+1} = T^n + \frac{\Delta t}{2} [23f(T^n, t^n) - 16f(T^{n-1}, t^{n-1}) + 5f(T^{n-2}, t^{n-2})] + \frac{\Delta t}{2} [g(T^{n+1}, t^{n+1}) + g(T^n, t^n)]$$

AB3 - explicit AM2 - implicit

Or as implemented

$$T^{n+1} = \left[T^n + \frac{\Delta t}{2} [23f(T^n, t^n) - 16f(T^{n-1}, t^{n-1}) + 5f(T^{n-2}, t^{n-2})] + \frac{\Delta t}{2} g(T^n, t^n) \right] \left(I - \frac{\Delta t}{2} g(T^n, t^n) \right)^{-1}$$

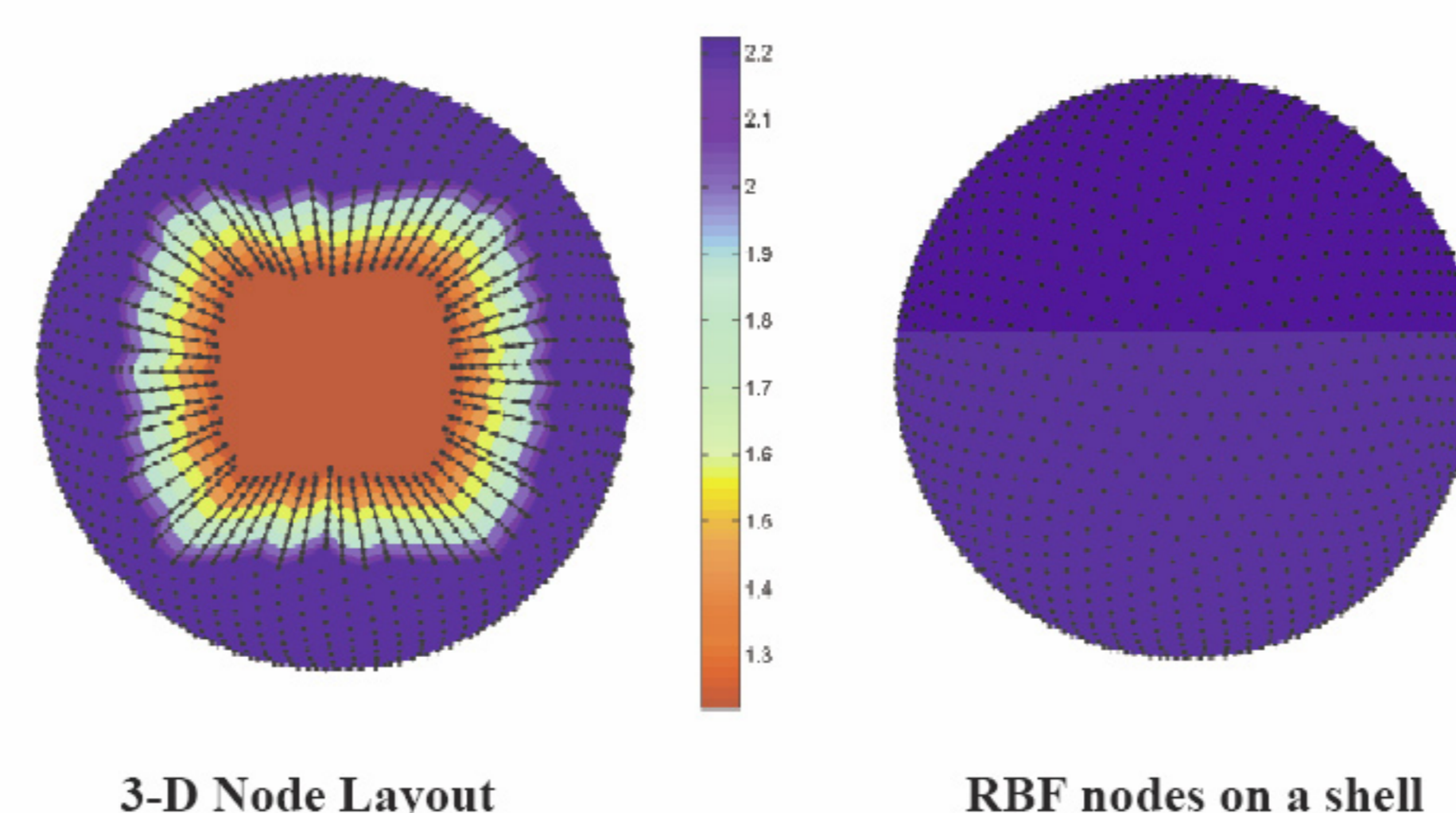
where $(I - \frac{\Delta t}{2} g(T^n, t^n))$ has been LU decomposed as a pre-processing step. The operators in r (such as in $g(T^n, t^n)$) have been spatially discretized with Chebyshev polynomials and those in θ, φ with RBFs,

Total Cost per time step: $O(N^2 M) + O(M^2 N) + O(N^2)$

Node Layout

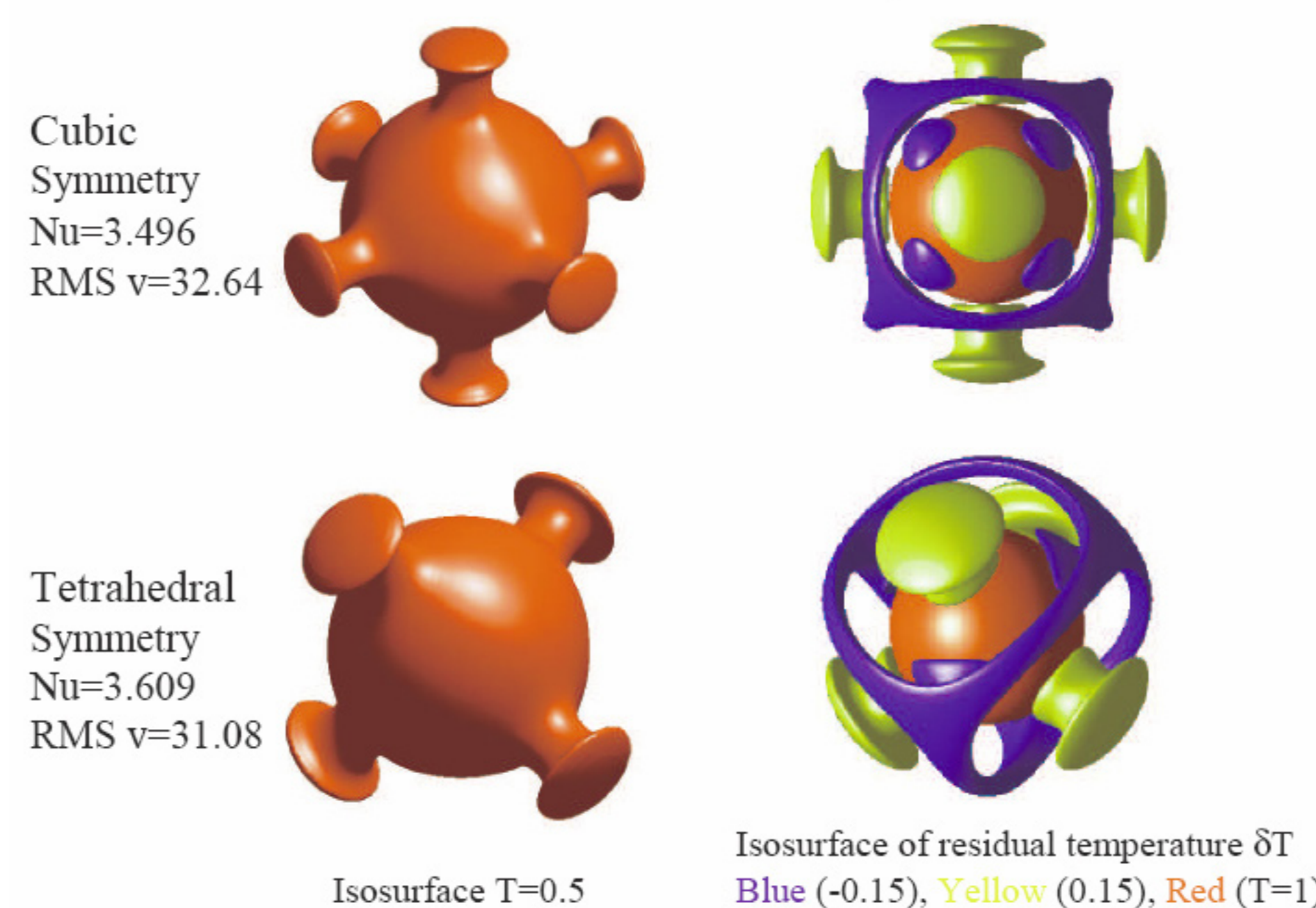
N = Number of RBF nodes on each spherical shell (θ and φ directions)

M = Number of Chebyshev nodes in radial direction



Numerical Results

Ra = 7000 N=1849 M=31 time/delta t = 0.24s (2.66GHz Intel Xeon X5335 6 cores)



Comparison with Other Numerical Methods for Ra = 7000

Model	Type	No. of Nodes	Nu _{outer}	<V _{rms} >	<T>
Tetrahedral					
Zhong [1]	FE	393,216	3.5126	32.66	0.2171
Kameyama [2]	FD	12,582,912	3.4945	32.6308	0.21597
Stemmer [3]	FV	663,552	3.4864	32.5894	0.21564
Harder [3]	SP-FD	552,960	3.4955	32.6375	0.21561
Harder [3]	SP-FD	Extrapolated*	3.4962	32.6424	0.21556
RBF	Pure SP	57,319	3.4962	32.6425	0.21556
Cubic					
Zhong [1]	FE	393,216	3.6254	31.09	0.2176
Kameyama [2]	FD	12,582,912	3.4945	32.6308	0.21597
Stemmer [3]	FV	663,552	3.5983	31.0226	0.21594
Harder [3]	SP-FD	552,960	3.6086	31.0765	0.21582
Harder [3]	SP-FD	Extrapolated*	3.6096	31.0821	0.21578
RBF	Pure SP	57,319	3.6096	31.0823	0.21578

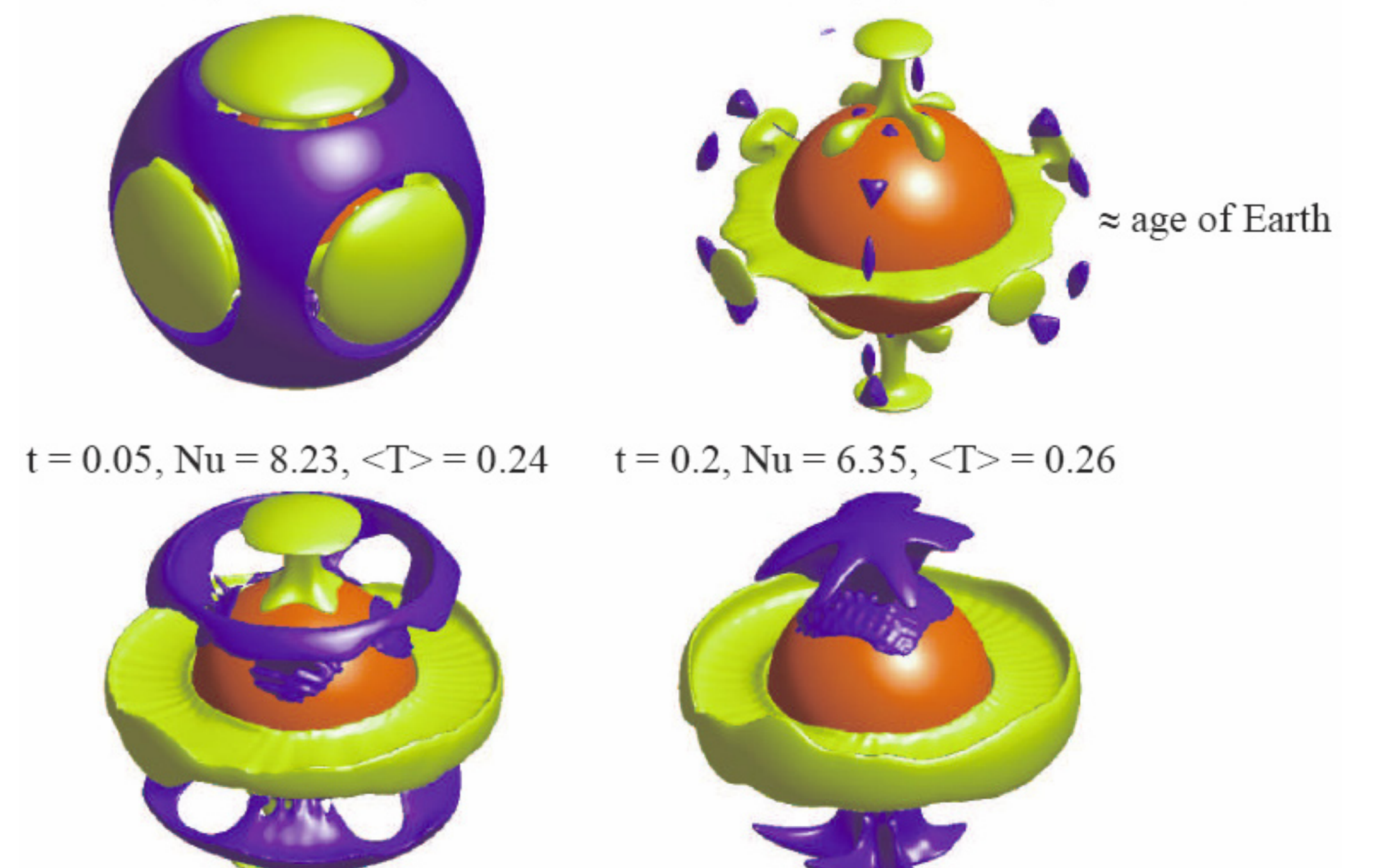
SP=Spectral, FD=Finite Difference, FV = Finite Volume, FE = Finite Element

* Results extrapolated from the 552,960 SP-FD Harder model, based on the known convergence rate of the scheme

Numerical Results for Ra=70000

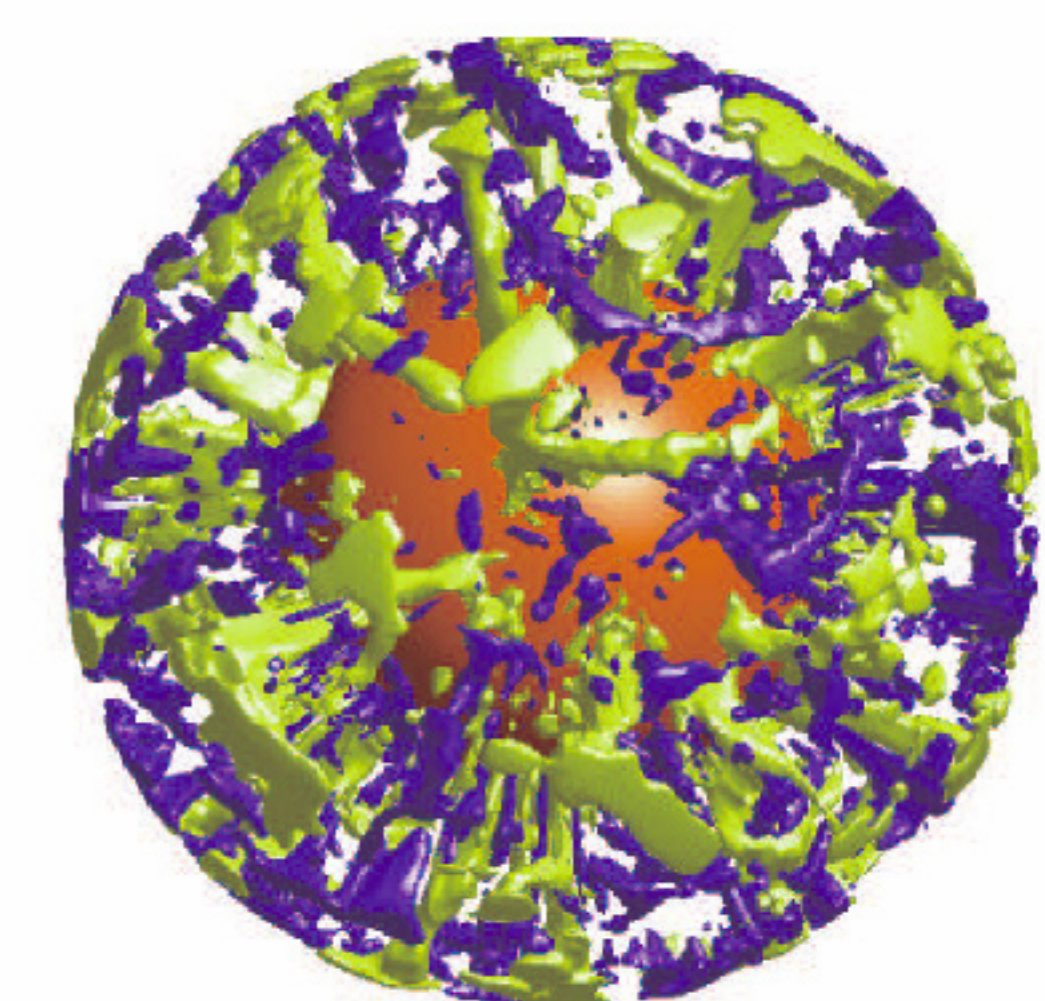
N=4096 M=51 time/delta t = 0.60s

T = 0.0036, Nu = 17.27, <T> = 0.31 t = 0.0172, Nu = 4.91, <T> = 0.26



Numerical Results for Ra=500,000

Nu = 14.46, RMS v = 251



References:

- S. Zhong, A. McNamara, E. Tan, L. Moresi, M. Gurnis, A benchmark study on mantle convection in a 3-D spherical shell using CitComS, *Geochim. Geophys. Geosyst.*, 9 (2008), no. 10.
- M.C. Kameyama, A. Kageyama, and T. Sato, Multigrid based simulation code for mantle convection in spherical shell using Yin-Yang grid, *Phys. Earth Planet. Interiors*, 171 (2008), 19-32.
- K. Stemmer, H. Harder, and U. Hansen, A new method to simulate convection with strongly temperature-dependent and pressure-dependent viscosity in spherical shell, *Phys. Earth Planet. Inter.*, 157 (2006), 223-249